

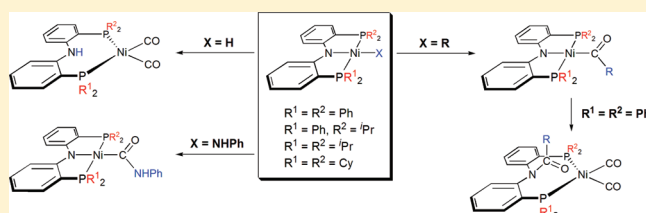
Divergent Carbonylation Reactivity Preferences of Nickel Complexes Containing Amido Pincer Ligands: Migratory Insertion versus Reductive Elimination

Lan-Chang Liang,* Yu-Ting Hung, Yu-Lun Huang, Pin-Shu Chien, Pei-Ying Lee, and Wei-Chen Chen

Department of Chemistry and Center for Nanoscience & Nanotechnology, National Sun Yat-sen University, Kaohsiung 80424, Taiwan

Supporting Information

ABSTRACT: The reactivity of a series of nickel(II) hydride, alkyl, and anilide complexes supported by amido diposphine ligands, including symmetrical $[N(o-C_6H_4PR_2)_2]^-$ ($R = Ph$ (**1a**), iPr (**1c**), Cy (**1d**)) and unsymmetrical $[N(o-C_6H_4PPh_2)(o-C_6H_4P^iPr_2)]^-$ (**1b**), with carbon monoxide is described. Exposure of a benzene solution of $[1a-d]NiH$ to carbon monoxide under ambient conditions leads to reductive elimination of diarylamine to give quantitatively zerovalent nickel dicarbonyl complexes $[H\cdot 1a-d]Ni(CO)_2$ (**2**). Migratory insertion of CO into the Ni-R bonds of $[1]NiR$ in benzene solutions affords Ni(II)-acyl derivatives $[1]NiC(O)R$ ($R = Me$ (**3**), Et (**4**), n -hexyl (**5**), 2-norbornyl (**6**)). Interestingly, further carbonylation of acyl **3a** and **4a** generates $[RC(O)N(o-C_6H_4PPh_2)_2]Ni(CO)_2$ ($R = Me$ (**7a**), Et (**8a**)) as a result of C–N bond-forming reductive elimination whereas no reaction occurs for **3b–c** or **4b–c** under similar conditions. Carbonylation of the anilide complexes $[1]NiNHPH$ produces carbamoyl $[1]Ni[C(O)NHPH]$ (**9**) as the final product irrespective of the identity of the phosphorus substituents. The decisive factors on the generation of these divergent carbonylation products are discussed.



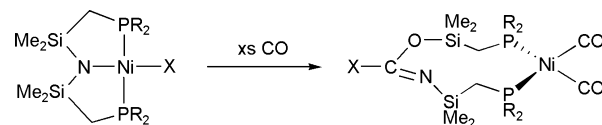
INTRODUCTION

Migratory insertion of carbon monoxide into a reactive transition-metal–ligand bond is of fundamental and commercial importance. These reactions are particularly relevant to catalytic olefin hydroformylation,¹ olefin/CO copolymerization,^{2–5} Monsanto acetic acid process,⁶ water-gas shift reactions,⁷ and thioester formation in Acetyl coenzyme A synthase,^{8–10} etc. Application of CO insertion chemistry has also proven essential in a variety of multiple-component reactions for the construction of carbonyl containing molecules such as amides,¹¹ lactones,^{12,13} acid anhydrides,¹⁴ ketones,^{15,16} and thiocarbamates,¹⁷ etc. In addition to the carbonylation step, oxidative addition and reductive elimination are often accompanied in these catalytic transformations. Understanding the decisive factors that control the efficacy of each of these elementary steps under carbonylation conditions is thus vital.

We are currently investigating reaction chemistry employing metal complexes of diarylamido phosphine ligands.^{18–28} Complexes of this type have recently received increasing attention.^{29–46} In particular, a series of hydridonickel(II) complexes of symmetrical $[N(o-C_6H_4PR_2)_2]^-$ ($R = Ph$ (**1a**), iPr (**1c**), Cy (**1d**)) and unsymmetrical $[N(o-C_6H_4PPh_2)(o-C_6H_4P^iPr_2)]^-$ (**1b**) are known to undergo olefin insertion reactions,⁴⁷ generating $[PNP]^-$ ligated organonickel(II) derivatives that are markedly thermally stable and resistant to β -elimination even at elevated temperatures.^{48,49} Given the widespread applications of carbonylation to synthetic chemistry, we are also interested in the reactivity studies of these

$[PNP]^-$ nickel(II) complexes with respect to carbon monoxide. Fryzuk et al. have previously demonstrated that hydrocarbylnickel(II) complexes $NiX[N(SiMe_2CH_2PR_2)_2]$ ($R = Ph$, $X = Me$, vinyl, allyl, Ph ; $R = Me$, $X = Ph$) react with CO to give $Ni(CO)_2[R_2PCH_2SiMe_2OC(X)=NSiMe_2CH_2PR_2]$ after a sequence of successive transformations including migratory insertion, reductive elimination, and N,O-silatripoc rearrangement (Scheme 1).^{50–52} Note that the formation of the

Scheme 1



nickel(0) dicarbonyl products in these reactions is independent of the identity of R or X incorporated. In this contribution, we show that the carbonylation reactivity of analogous *o*-phenylene derived $[PNP]^-$ complexes is, in contrast to that of $[N(SiMe_2CH_2PR_2)_2]^-$ derivatives, a function of the characteristics of the phosphorus substituents and the nickel-bound hydro(carbyl) ligand. Without the incorporation of the N–Si bonds in $[PNP]^-$, the transformations reported herein thus prohibit N,O-silatripoc rearrangement. The possibilities of CO

Received: October 27, 2011

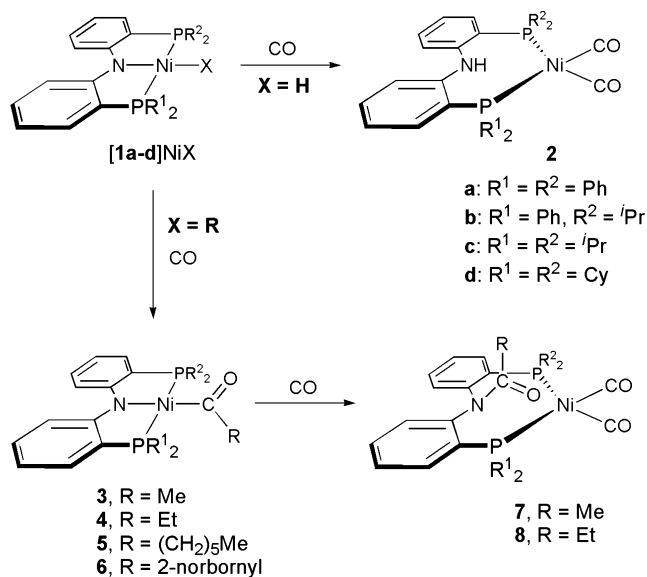
Published: December 30, 2011

insertion and/or CO induced reductive elimination involving Ni–H, Ni–C, and Ni–N bonds are discussed.

RESULTS AND DISCUSSION

Scheme 2 summarizes the carbonylation of [1]NiX (X = H, alkyl) under ambient conditions. Treating a benzene solution of

Scheme 2



[1a–d]NiH^{47,53} with an atmosphere of carbon monoxide at room temperature led to the generation of diamagnetic, colorless or pale yellow crystalline [H·1a–d]Ni(CO)₂ (**2a–d**) in high isolated yield. No CO insertion product, i.e., formyl complexes,^{54–57} was detectable by ¹H or ³¹P{¹H} NMR spectra. Upon carbonylation, the characteristic hydride resonance of [1]NiH at –18 ppm disappears gradually in the ¹H NMR spectra to give instead a new signal at 9–11 ppm with *J*_{HP} of ~10 Hz because of the formation of an N–H bond (Table 1). The observed NH and ³¹P chemical shifts of **2** are all

relatively downfield as compared to those of the corresponding H[1] (δ_{NH} ranging from 6.7 to 8.5 ppm; δ_{P} ranging from ca. –13 to –22 ppm).^{47–49} The coordination of terminal carbonyl ligands in **2** is confirmed by the observation of a diagnostic signal at ~200 ppm with ²*J*_{CP} of 5 Hz in the ¹³C NMR and two C–O stretching bands at ~2000 and 1930 cm^{–1} in the infrared spectra. The formation of the zerovalent nickel dicarbonyl complexes **2** is obviously a consequence of reductive elimination of diarylamine from [1]NiH upon carbonylation. These results are intriguing as the divalent nickel hydride complexes [1]NiH were readily produced (quantitatively less than 10 min) by oxidative addition of Ni(COD)₂ with H[1].^{47,53} We note that [1c]NiH is thermally stable; no decomposition was observed by ¹H or ³¹P{¹H} NMR when a benzene solution of [1c]NiH (57 mmol) was heated at 100 °C for 4 days. The N–H bond-forming reductive elimination from [1]NiH is thus apparently triggered by prior CO coordination rather than thermal decomposition. This result is ascribable to an increase in electrophilicity of a metal due to the ligation of a strong π acid. In comparison, no reductive elimination was found for [1]NiH upon reactions with relatively weak π acceptors, such as olefins.⁴⁷

The solid-state structures of **2b** and **2c** were established crystallographically. The molecular structure of **2b** is depicted in Figure 1. As illustrated, the nickel center is surrounded by two phosphorus donors and two terminal carbonyl ligands with the geometry being best described as distorted tetrahedral. The core geometry of **2c** (Supporting Information Figure S1) resembles closely that of **2b**. The Ni–P, Ni–C, and C–O distances and the bond angles about nickel are all typical for a Ni(0) dicarbonyl diphosphine complex.^{10,59,60} Selected bond distances and angles are summarized in Tables 2 and 3.

Unlike the hydride [1]NiH, the alkyl complexes [1]NiR undergo CO migratory insertion involving the Ni–R bond to produce the corresponding acyl derivatives [1]NiC(O)R (R = Me (**3**), Et (**4**), *n*-hexyl (**5**), 2-norbornyl (**6**)). In general, these reactions proceed cleanly to give the insertion products in few hours under ambient conditions; no N–C_{sp3} bond-forming reductive elimination occurs.⁶¹ It is likely that the more

Table 1. Selected NMR and IR Spectroscopic Data^a

compound	δ_{NH}	δ_{P}	² <i>J</i> _{PP}	$\delta_{\text{C}\alpha}$	² <i>J</i> _{PCα}	$\nu(\text{C}\equiv\text{O})$	$\nu(\text{C}=\text{O})$
2a	8.61	16.2		199.4	4.5	1993, 1924	
2b	9.99	23.7, 13.7		200.4	4.6	2004, 1948	
2c	10.65	19.3		201.6	5.0	2000, 1942	
2d	10.63	9.8		201.9	5.5	1997, 1937	
3a		18.8					
3b		37.8, 18.3	192	259.7	18.8		1621 ^c
3c		35.8		259.2	20.5		1618
4a		16.0					
4b		36.9, 17.6	194	261.2	19.2		1622 ^c
4c		35.6		259.3	20.6		1618 ^c
5b		36.9, 17.9	193	260.8	18.8		1621 ^c
6b		34.8, 18.2	194	264.1	18.3		1621 ^c
7a		23.4, 22.2	5.6	197.2	4.5	2002, 1943 ^c	1695 ^c
8a		24.7, 23.5	5.5	197.9	6.0	1994, 1927	1693
9a	6.77	22.3		194.5	31.0		1558 (1573) ^c
9b	6.89 ^b	42.8, 21.1 ^b	222 ^b	195.7 ^b	27.0 ^b		1572 (1585) ^c
9c	7.19	40.9		196.1	27.4		1572

^aUnless otherwise noted, all NMR spectra were recorded in C₆D₆ at room temperature, chemical shifts in ppm, coupling constants in Hz; all IR spectra were recorded in Nujol at room temperature, stretching frequency in cm^{–1}. ^bData selected from ref 58. ^cData recorded in THF.

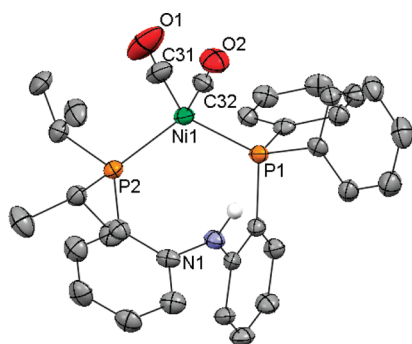


Figure 1. Molecular structure of **2b** with thermal ellipsoids drawn at the 35% probability level. All hydrogen atoms (except NH) and one benzene molecule present in the asymmetric unit cell are omitted for clarity.

Table 2. Selected Bond Distances (Å) for **2b**, **2c**, and **8a**

compound	Ni–P	Ni–C	C≡O	C=O
2b	2.2425(19), 2.248(2)	1.756(10), 1.796(9)	1.139(10), 1.122(9)	
2c^a	2.285(3), 2.286(3)	1.800(14), 1.833(17)	1.089(17), 1.104(16)	
8a	2.2139(8), 2.2151(8)	1.768(4), 1.768(3)	1.149(3), 1.151(4)	1.210(3)

^aThe data summarized represent one of two independent molecules found in the asymmetric unit cell.

Table 3. Selected Bond Angles (deg) for **2b**, **2c**, and **8a**

compound	P–Ni–P	C–Ni–C	P–Ni–C	Ni–C≡O
2b	118.41(7)	114.3(4)	106.3(3), 107.2(2), 103.8(3), 107.1(2)	177.2(9), 177.9(7)
2c^a	120.68(13)	110.2(6)	100.3(4), 110.7(4), 109.3(4), 105.4(4)	177.0(14), 176.0(13)
8a	110.01(3)	110.54(14)	105.49(11), 108.57(10), 104.17(11), 117.39(9)	171.4(3), 178.5(3)

^aThe data summarized represent one of two independent molecules found in the asymmetric unit cell.

electron-releasing nature of alkyl ligands makes $[1]NiR$ more reluctant to reductive elimination than $[1]NiH$. In contrast, no reaction was observed for $[1]NiPh$ ^{48,49,53} under similar conditions unless after a prolonged period of time as evidenced by $^{31}P\{^1H\}$ NMR,⁶² indicating that migratory insertion of CO into a Ni–C_{sp2} bond proceeds much slower than that involving Ni–C_{sp3}.⁶³ Introduction of carbon monoxide (ca. 5 equiv) to a benzene solution containing $[1]NiH$ and an excess amount of olefin (e.g., 5 equiv) also generates cleanly the corresponding acyl complexes; no N–H bond-forming reductive elimination product **2** was detectable by $^{31}P\{^1H\}$ NMR. This result implies that olefin insertion into the Ni–H bond of $[1]NiH$ proceeds at a much faster rate than the N–H bond-forming reductive elimination under carbonylation conditions. We note that **2** does not react with olefins, thus ruling out the possibility of reversible reductive elimination/oxidative addition involving $[1]NiH$ and **2**, respectively, followed by sequential olefin and CO insertion. These reactions are particularly relevant to catalytic olefin/CO copolymerization,^{2–5} though in the current study olefins appear not to effectively insert into the Ni–acyl bond. Interestingly, solution $^{31}P\{^1H\}$ NMR studies on carbonylation of $[1a]NiR$ (R = Me, Et) revealed that $[1a]NiC(O)R$ (**3a/4a**) is an intermediate that is always

accompanied by either $[1a]NiR$ or the final product $[RC(O)N(o-C_6H_4PPh_2)_2]Ni(CO)_2$ (R = Me (**7a**), Et (**8a**)) throughout the reaction. The ^{31}P chemical shifts of **3a** (δ_P 19) and **4a** (δ_P 16) are comparable to those corresponding to the phenyl-substituted phosphorus atom in **3b** and **4b**, respectively (Table 1). This phenomenon is reminiscent of the established organonickel chemistry involving $[1a]^-$, $[1b]^-$, and $[1c]^-$.⁴⁷ Complexes **7a** and **8a** are zerovalent nickel dicarbonyls similar to **2**, though the diphosphine ligands in the former are amide functionalized due to N–C_{sp2} bond-forming reductive elimination involving Ni–N and Ni–acyl bonds. This result is interesting in view of the fact that neither N–C_{sp3} nor N–C_{sp2} bond-forming reductive elimination occurs for the hydrocarbyl complexes $[1a]NiR$ (R = Me, Et, Ph) under similar conditions, highlighting the higher reactivity of the Ni–acyl bond to undergo reductive elimination due to increased electrophilicity induced by the high electronegative acyl oxygen atom. In contrast to **3a** and **4a**, no reaction was found for **3b–c** or **4b–c** upon carbonylation, even after a prolonged period of time (>4 days). The discrepancy in carbonylation reactivity of **3a** and **4a** versus **3b–c** and **4b–c** thus underscores the phosphorus substituent effect in the amido pincer ligands $[1]^-$ on N–C_{sp2(acyl)} bond-forming reductive elimination. In general, these acyl complexes remain intact even at elevated temperatures on the basis of $^{31}P\{^1H\}$ NMR studies; for instance, no decomposition was found when a benzene solution of **4c** (46 mM) was heated to 80 °C for 10 days. Though **3a** and **4a** were not isolated, their thermal stability is presumably similar to that of **3b–c** and **4b–c**. The reductive elimination reactivity found for **3a** and **4a** in the presence of carbon monoxide should thus be initiated by CO coordination to form five-coordinate⁶⁴ intermediates **3a**·CO and **4a**·CO, respectively, taking into account the nondissociative nature of $[1]^-$.^{47–49} With the incorporation of more electron-releasing phosphorus-bound isopropyl substituents in $[1b–c]^-$, the metal center in acyl **3b–c** and **4b–c** is less electrophilic, even with the ligation of a strong π acidic CO, and thus more reluctant to reductive elimination. Interestingly, the reactivity similarity of $[1b]^-$ complexes to $[1c]^-$ instead of $[1a]^-$ derivatives upon carbonylation described herein is notably different from what was found in the established olefin insertion chemistry, where the reactivity of $[1b]NiH$ resembles that of $[1a]NiH$ instead of $[1c]NiH$.⁴⁷ On steric grounds, ligands with bulky substituents should encourage reductive elimination. The fact that $[1a]^-$ complexes rather than sterically more demanding $[1b]^-$ and $[1c]^-$ derivatives undergo reductive elimination suggests electronic factors predominate in these transformations. Note that with the incorporation of a sterically demanding acyl ligand, **6b** does not undergo reductive elimination in the presence of CO.

The solution NMR and infrared spectroscopic data of **3–6** are all consistent with a constitution having a nickel-bound acyl ligand in these molecules. The characteristic acyl carbonyl carbon resonance is observed in the ^{13}C NMR spectra at ca. 260 ppm, a value that is markedly downfield shifted as compared to those of the terminal carbonyl ligands in **2**. The $^2J_{CP}$ coupling constants of ~20 Hz observed for **3–6** are significantly larger than those of tetrahedral **2** but well within the range expected for square planar organonickel(II) complexes of $[PNP]^-$ ligands.^{47–49} The infrared spectra of **3–6** show a carbonyl band at ca. 1620 cm⁻¹, diagnostic of an acyl C=O stretching frequency. Reminiscent of the established $[1]NiR$,^{47–49} the amido diphosphine ligands of **3–6** are

meridionally bound to nickel as evidenced by virtual triplet resonances observed in the $^{13}\text{C}\{^1\text{H}\}$ NMR spectra for the *o*-phenylene carbon atoms in $[\mathbf{1c}]^-$ complexes and somewhat large $^2J_{\text{PP}}$ values of ca. 193 Hz found in the $^{31}\text{P}\{^1\text{H}\}$ NMR spectra for the unsymmetrically substituted phosphorus atoms in $[\mathbf{1b}]^-$ derivatives. The two phosphorus atoms in $[\mathbf{1a}]^-$ and $[\mathbf{1c}]^-$ derived acyl complexes are chemically equivalent on the NMR time scale.

The acyl complexes **3b**, **3c**, **5b**, and **6b** were also characterized by X-ray diffraction analysis. As depicted in Figures 2–5, these complexes are four-coordinate species with

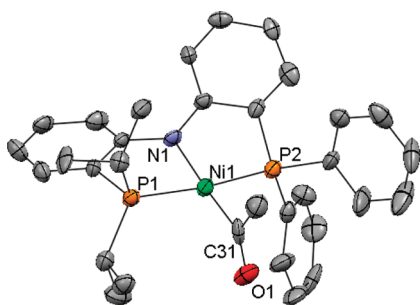


Figure 2. Molecular structure of **3b** with thermal ellipsoids drawn at the 35% probability level. All hydrogen atoms and one unbound THF present in the asymmetric unit cell are omitted for clarity.

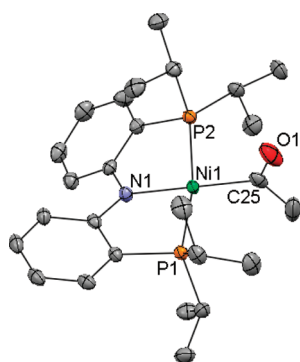


Figure 3. Molecular structure of **3c** with thermal ellipsoids drawn at the 35% probability level. All hydrogen atoms are omitted for clarity.

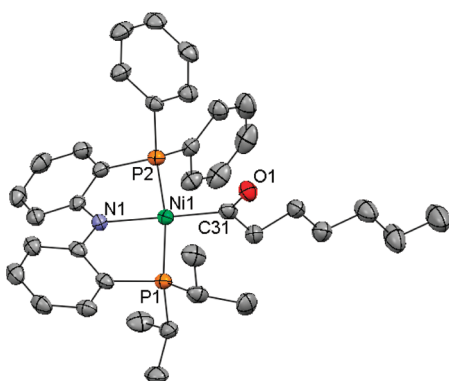


Figure 4. Molecular structure of **5b** with thermal ellipsoids drawn at the 35% probability level. All hydrogen atoms and one benzene molecule present in the asymmetric unit cell are omitted for clarity.

the amido diphosphine ligands being meridionally bound to the nickel center, consistent with the solution structure determined by NMR studies. In general, the nickel atom in these acyl

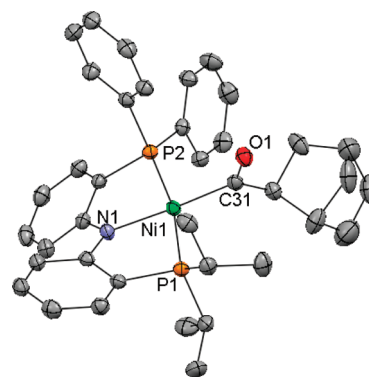


Figure 5. Molecular structure of **6b** with thermal ellipsoids drawn at the 35% probability level. All hydrogen atoms and one benzene molecule present in the asymmetric unit cell are omitted for clarity.

complexes lies perfectly on the square planar coordination plane. The geometry of the sp^2 -hybridized carbonyl carbon atom is trigonal planar. The acyl ligand is oriented such that the $\text{O}=\text{C}_\alpha\text{-C}_\beta$ plane is roughly orthogonal to the mean coordination plane, consistent with what is expected from the steric standpoint. Selected bond distances and angles of these acyl complexes are summarized in Tables 4 and 5. Though

Table 4. Selected Bond Distances (Å) for **3b**, **3c**, **5b**, **6b**, **9a**, and **9c**

compound	Ni–N	Ni–C	Ni–P	C=O
3b	1.982(11)	1.891(17)	2.159(4), 2.174(4)	1.184(17)
3c	1.9522(17)	1.890(2)	2.1718(6), 2.1772(6)	1.187(3)
5b	1.967(3)	1.873(4)	2.1685(11), 2.1698(11)	1.211(5)
6b	1.974(3)	1.886(4)	2.1782(10), 2.1899(10)	1.218(5)
9a	1.934(3)	1.881(4)	2.1627(10), 2.1710(10)	1.223(4)
9c^a	1.948(18)	1.89(2)	2.173(7), 2.200(7)	1.25(2)

^aThe data summarized represent one of two independent molecules found in the asymmetric unit cell.

these values are all well within the expected ranges, the Ni–C distances reported herein are shorter by $\sim 0.05\text{--}0.11$ Å than those of their corresponding alkyl precursors,⁶⁵ reflective of the intrinsic differences in atomic sizes of sp^2 - versus sp^3 -hybridized carbon atoms. Nevertheless, the acyl ligands exhibit approximately the same trans influence as alkyls as evidenced by the corresponding Ni–N distances. The Ni–C=O angles are decreased with increased steric sizes of the hydrocarbyl substituent in the acyl ligands as indicated by a series of $[\mathbf{1b}]^-$ derivatives characterized.

Unlike acyl **3a** and **4a**, both **7a** and **8a** exhibit two doublet resonances in the $^{31}\text{P}\{^1\text{H}\}$ NMR spectra for the phosphorus atoms, indicating dissymmetrization of this diphosphine ligand upon $\text{N-C}_{\text{sp}^2(\text{acyl})}$ bond-forming reductive elimination. In **8a**, the methylene protons in the amide group –NC(O)Et are diastereotopic as indicated by two multiplet resonances observed at 2.29 and 2.16 ppm in the ^1H NMR spectrum. Note that the two phosphorus atoms in **2a** are chemically equivalent on the NMR time scale. The lower symmetry observed for **7a** and **8a** than for **2a** is apparently a consequence of larger N-substituents in the diphosphine ligands derived. The low $^2J_{\text{PP}}$ values of ca. 6 Hz found for **7a** and **8a** are consistent

Table 5. Selected Bond Angles (deg) for 3b, 3c, 5b, 6b, 9a, and 9c

compound	N–Ni–P	P–Ni–P	P–Ni–C	N–Ni–C	Ni–C=O
3b	85.2(4), 86.1(3)	171.29(18)	93.1(4), 95.7(4)	177.1(6)	126.4(13)
3c	85.17(5), 85.92(5)	167.61(2)	94.24(7), 94.87(7)	178.48(9)	122.8(2)
5b	85.28(10), 85.24(10)	168.97(5)	93.90(12), 95.58(12)	179.18(15)	123.1(4)
6b	83.55(9), 84.53(9)	167.98(4)	94.46(11), 97.39(11)	177.08(15)	120.7(3)
9a	82.90(9), 86.28(9)	163.74(4)	95.77(12), 95.50(12)	177.31(15)	124.4(3)
9c ^a	85.1(6), 85.1(6)	165.7(3)	92.7(7), 95.6(7)	172.3(9)	120.5(17)

^aThe data summarized represent one of two independent molecules found in the asymmetric unit cell.

with two cis-disposed phosphorus atoms in these molecules. In the ¹³C NMR spectra of 7a and 8a, the terminal carbonyl carbon resonance is observed at 197 ppm whereas the amide carbonyl is at 202 ppm. The infrared spectra of 7a and 8a show CO stretching bands at ca. 2000 and 1930 cm⁻¹ for the terminal ligands and ca. 1693 cm⁻¹ for the amide group. It is interesting to note that the single ¹³C NMR signal found for the terminal carbonyl carbon atoms in 2a–d, 7a, and 8a implies presumably rapid inversion at the pyramidal diarylamino nitrogen, which is somewhat unusual particularly for 7a and 8a that carry a relatively large N-substituent.

Figure 6 depicts the X-ray structure of 8a. Similar to 2b and 2c derived from reductive elimination, 8a contains a

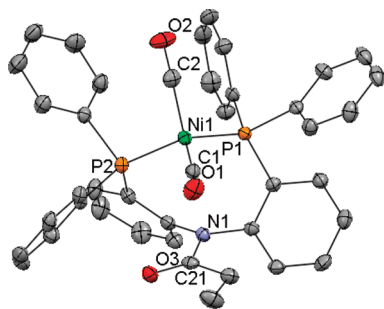
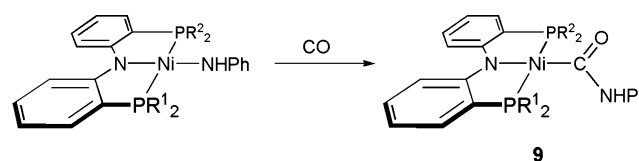


Figure 6. Molecular structure of 8a with thermal ellipsoids drawn at the 35% probability level. All hydrogen atoms and one benzene molecule present in the asymmetric unit cell are omitted for clarity.

tetrahedral, zerovalent nickel core supported by two phosphorus donors and two carbonyl ligands. The mono-anionic [1a]⁻ ligand in the precursor complex 4a has transformed upon carbonylation to become a neutral diphosphine chelate functionalized with one amide group. As expected, the C–O distances in terminal carbonyls are shorter than that in the amide group (Table 2). The amide –C(O)N– group is nearly coplanar. The Ni–C1–O1 angle of 171.4(3)^o (Table 3) is markedly deviated from the ideal linearity due to steric repulsion arisen from the amide group.

In principle, compounds 7a and 8a may be alternatively produced by CO insertion into the Ni–N bond of [1a]NiR followed by C_{sp2}–C_{sp3} bond-forming reductive elimination. Though this is not the case found in this study, we are interested to evaluate the possibilities of CO insertion into a nickel–amide bond. In this regard, the carbonylation reactivity of [1]NiNHPh^{58,66} that contains an unsupported Ni–N bond was examined. Though not unprecedented, CO insertion into a late-transition-metal–amide bond is uncommon.^{67,68} Exposure of a benzene solution of [1a–c]NiNHPh to an atmosphere of CO at room temperature results in the formation of the corresponding carbamoyl complexes [1a–c]Ni[C(O)NHPh] (9a–c) in high isolated yield (Scheme 3). Notably, only the

Scheme 3



terminal Ni–N bond in [1]NiNHPh is involved in these reactions, indicating that a nickel–amide bond is indeed reactive toward CO insertion but the lack of reactivity of that involving [1]⁻ is a consequence of chelate effect. In contrast to the acyl 3a and 4a, the carbamoyl complexes 9 do not undergo N–C_{sp2} bond-forming reductive elimination in the presence of CO. The discrepancy in reactivity of 9a versus 3a and 4a is ascribed to lower electrophilicity of the former due to the participation of a nitrogen lone electron pair in carbamoyl –C(O)N– π resonance. These carbamoyl complexes are thermally stable; neither decarbonylation nor β -elimination was observed even at elevated temperatures. For instance, [1c]Ni[C(O)NHPh] (40 mM in benzene) remains intact upon heating to 110 °C for 4 days as evidenced by ³¹P{¹H} NMR spectroscopy.

The NMR and infrared spectroscopic data of 9a–c are all consistent with the formation of a carbamoyl ligand in these molecules. Upon carbonylation, the characteristic NH resonance of [1]NiNHPh at ca. –1.2 ppm moves downfield to ca. 7.0 ppm in the ¹H NMR spectra. The carbonyl carbon resonance is observed in the ¹³C NMR spectra at ~196 ppm, a value that is significantly upfield shifted as compared to those of the acyl 3–6. The C=O stretching frequencies of 9, as determined by IR spectroscopy at ~1570 cm⁻¹, are lower than those of 3–6, consistent with the occurrence of π resonance in carbamoyl –C(O)N– moiety of the former complexes.

Compounds 9a and 9c were also characterized crystallographically. As illustrated in Figure 7, 9a contains a nickel-bound carbamoyl ligand. The Ni–P, Ni–N, and Ni–C_{sp2} distances (Table 4) and the bond angles about nickel (Table 5) are all typical for a square planar nickel(II) derivatives. Notably, the Ni–N distance of 9a is comparable to those of [1]NiR and [1]NiC(O)R, indicating that the trans influence of the carbamoyl ligand is nearly identical to those of alkyls and acyls. The core geometry of 9c (Supporting Information Figure S2) is similar to that of 9a, though 9c crystallizes as a dimer linked with hydrogen bonds between carbamoyl groups (Supporting Information Figure S3).

CONCLUSIONS

We have demonstrated that the product constitution of carbonylation of [PNP]NiX (X = hydride, alkyl, and amide) is governed by the characteristics of the phosphorus substituents and the identity of the nickel-bound X ligands. These results are notably different from those derived from

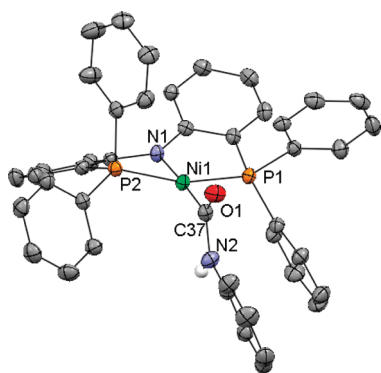


Figure 7. Molecular structure of **9a** with thermal ellipsoids drawn at the 35% probability level. All hydrogen atoms (except NH) and one unbound THF present in the asymmetric unit cell are omitted for clarity.

analogous $[\text{N}(\text{SiMe}_2\text{CH}_2\text{PR}_2)_2]^-$ complexes.^{50–52} In the presence of carbon monoxide, the hydride complexes $[\mathbf{1}]NiH$ undergo exclusively N–H bond-forming reductive elimination to generate zerovalent nickel dicarbonyl **2** whereas the anilide $[\mathbf{1}]NiNHP$ prefer migratory insertion to give nickel(II) carbamoyl derivatives **9**. Interestingly, though all alkyl complexes $[\mathbf{1a-c}]NiR$ react with CO to produce acyl $[\mathbf{1a-c}]NiC(O)R$, it is the phenyl substituted $[\mathbf{1a}]^-$ derivatives that undergo subsequent N–C_{sp2} bond-forming reductive elimination to afford **7** and **8**, where the nickel-bound diphosphine ligands are amide functionalized. These reactivity preferences are clearly a function of the electrophilicity of the metal center involved. These results are particularly relevant to the synthesis of carbonyl containing organic molecules via successive oxidative addition, CO migratory insertion, and reductive elimination.

EXPERIMENTAL SECTION

General Procedures. Unless otherwise specified, all experiments were performed under nitrogen using standard Schlenk or glovebox techniques. All solvents were reagent grade or better and purified by standard methods. The NMR spectra were recorded on Varian Unity or Bruker AV instruments. Chemical shifts (δ) are listed as parts per million downfield from tetramethylsilane. Coupling constants (J) are listed in hertz. ¹H NMR spectra are referenced using the residual solvent peak at δ 7.16 for C₆D₆. ¹³C NMR spectra are referenced using the internal solvent peak at δ 128.39 for C₆D₆. The assignment of the carbon atoms for all new compounds is based on the DEPT ¹³C NMR spectroscopy. ³¹P NMR spectra are referenced externally using 85% H₃PO₄ at δ 0. Routine coupling constants are not listed. All NMR spectra were recorded at room temperature in specified solvents unless otherwise noted. The infrared spectra were recorded in Nujol mulls or THF solutions between KBr plates on Varian 640-IR FT-IR spectrometer. Elemental analysis was performed on a Heraeus CHN-O Rapid analyzer.

Materials. Compounds $[\mathbf{1a-d}]NiH$,^{47,53} $[\mathbf{1a}]NiMe$,^{48,49} $[\mathbf{1c}]NiMe$,⁴⁹ $[\mathbf{1a-c}]NiEt$,^{47,49} $[\mathbf{1b}]Ni(n\text{-hexyl})$,⁴⁷ $[\mathbf{1b}]Ni(2\text{-norbornyl})$,⁴⁷ $[\mathbf{1b}]NiCl$,⁵⁸ and **9b**⁵⁸ were prepared according to the procedures reported previously. All other chemicals were obtained from commercial vendors and used as received.

X-ray Crystallography. Supporting Information Table S1 summarizes the crystallographic data for all structurally characterized compounds. Data were collected on a Bruker-Nonius Kappa CCD diffractometer with graphite monochromated Mo- $K\alpha$ radiation (λ = 0.7107 Å). Structures were solved by direct methods and refined by full matrix least-squares procedures against F^2 using SHELXL-97.⁶⁹ All full-weight non-hydrogen atoms were refined anisotropically. Hydrogen atoms were placed in calculated positions. The crystals of **2c**, **8a**,

and **9c** were of poor quality but sufficient to establish the identity of these molecules.

Synthesis of $[\mathbf{1b}]NiMe$. To a THF solution (3 mL) of $[\mathbf{1b}]NiCl$ (165 mg, 0.29 mmol) at -35°C was added MeMgCl (0.1 mL, 3 M in THF, 0.3 mmol) dropwise. The reaction solution was stirred at room temperature for 2 h and evaporated to dryness in vacuo. The solid residue thus obtained was triturated with pentane (2 mL \times 2) and benzene (6 mL) was added. The benzene solution was filtered through a pad of Celite, which was further washed with benzene until the washings became colorless. The combined filtrate was evaporated to dryness in vacuo to afford the product as a red solid. Red crystals suitable for X-ray diffraction analysis were grown by layering diethyl ether on a concentrated THF solution at -35°C ; yield 130 mg (82%). The X-ray structure is depicted in Supporting Information Figure S4. ¹H NMR (C₆D₆, 500 MHz) δ 7.82 (dd, 1, Ar), 7.75 (m, 4, Ar), 7.12 (dt, 1, Ar), 7.07 (dt, 1, Ar), 7.03 (m, 7, Ar), 7.00 (q, 2, Ar), 6.52 (t, 1, Ar), 6.41 (t, 1, Ar), 2.10 (m, 2, CHMe₂), 1.22 (dd, 6, CHMe₂), 1.06 (dd, 6, CHMe₂), -0.09 (dd, 3, J = 8.5 and 9.5, NiMe). ³¹P{¹H} NMR (C₆D₆, 202 MHz) δ 37.73 (d, ²J_{PP} = 282.2, PⁱPr₂), 27.05 (d, ²J_{PP} = 282.2, PPh₂). ¹³C{¹H} NMR (C₆D₆, 125.7 MHz) δ 163.41 (dd, J_{CP} = 21.0 and 4.0, C), 163.18 (dd, J_{CP} = 25.1 and 3.3, C), 134.85 (s, CH), 134.04 (d, J_{CP} = 11.4, CH), 132.89 (dd, J_{CP} = 40.8 and 1.4, C), 132.52 (s, CH), 132.30 (d, J_{CP} = 1.4, CH), 131.59 (d, J_{CP} = 1.8, CH), 130.36 (d, J_{CP} = 2.4, CH), 129.19 (d, J_{CP} = 9.7, CH), 125.19 (d, J_{CP} = 45.7, C), 122.23 (d, J_{CP} = 36.5, C), 116.75 (d, J_{CP} = 16.1, CH), 116.74 (s, CH), 116.34 (d, J_{CP} = 5.5, CH), 115.71 (d, J_{CP} = 10.9, CH), 24.27 (dd, J_{CP} = 21.6 and 1.9, CHMe₂), 19.32 (d, J_{CP} = 5.0, CHMe₂), 18.30 (s, CHMe₂), -20.45 (dd, J_{CP} = 23.34 and 23.85, NiMe). Anal. Calcd. for C₃₁H₃₅NNiP₂: C, 68.65; H, 6.51; N, 2.58. Found: C, 68.27; H, 6.28; N, 2.74.

General Procedures for the Carbonylation of $[\mathbf{1}]NiX$ (X = H, Me, Et, *n*-hexyl, 2-norbornyl, NHPH). In a Teflon-capped reaction vessel (100 mL), a solution of $[\mathbf{1}]NiX$ (typically 0.2–0.5 mmol) in benzene (5 mL) was degassed with freeze–pump–thaw cycles (three times) and CO (1 atm) was introduced at room temperature. The reaction solution was stirred at room temperature for 4–24 h and evaporated to dryness under reduced pressure. The solid residue thus obtained was triturated with pentane (2 mL \times 2) and dried in vacuo.

Synthesis of $[\mathbf{H-1a}]Ni(CO)_2$ (2a**).** Isolated as a colorless crystalline solid; yield 94%. ¹H NMR (C₆D₆, 500 MHz) δ 8.61 (t, 1, J_{HP} = 7.0, NH), 7.53 (m, 8, Ar), 7.07 (m, 2, Ar), 6.98 (m, 12, Ar), 6.92 (td, 2, Ar), 6.82 (td, 2, Ar), 6.56 (t, 2, Ar). ³¹P{¹H} NMR (C₆D₆, 202 MHz) δ 16.16. ¹³C{¹H} NMR (C₆D₆, 125.7 MHz) δ 199.43 (t, ²J_{CP} = 4.5, NiCO), 149.98 (m, C), 136.77 (m, C), 134.26 (s, CH), 133.96 (m, CH), 131.04 (s, CH), 129.80 (s, CH), 128.90 (m, CH), 126.43 (m, C), 123.93 (t, J_{CP} = 2.4, CH), 123.46 (t, J_{CP} = 2.3, CH). Anal. Calcd for C₃₈H₂₉NNiO₂P₂: C, 69.95; H, 4.48; N, 2.15. Found: C, 69.80; H, 4.60; N, 2.04.

Synthesis of $[\mathbf{H-1b}]Ni(CO)_2$ (2b**).** Isolated as pale yellow crystals suitable for X-ray diffraction analysis by slow evaporation of a concentrated benzene solution at room temperature; yield 70%. ¹H NMR (C₆D₆, 500 MHz) δ 9.99 (vt, 1, J_{HP} = 9.8, NH), 7.60 (dd, 4, Ar), 7.26 (m, 2, Ar), 7.02 (m, 10, Ar), 6.80 (dd, 1, Ar), 6.65 (dd, 1, Ar), 2.02 (m, 2, CHMe₂), 1.05 (dd, 6, CHMe₂), 0.81 (dd, 6, CHMe₂). ³¹P{¹H} NMR (C₆D₆, 202 MHz) δ 23.67 (s, PⁱPr₂), 13.65 (s, PPh₂). ¹³C{¹H} NMR (C₆D₆, 125.7 MHz) δ 200.38 (vt, ²J_{CP} = 4.6, NiCO), 151.19 (d, J_{CP} = 11.4, C), 150.66 (d, J_{CP} = 13.2, C), 137.13 (dd, J_{CP} = 33.8 and 4.5, C), 134.46 (s, CH), 133.87 (d, J_{CP} = 13.3, CH), 132.59 (s, CH), 131.41 (s, CH), 130.44 (s, CH), 129.76 (s, CH), 128.92 (s, CH), 128.88 (d, J_{CP} = 3.8, CH), 123.30 (d, J_{CP} = 30.6, C), 123.25 (d, J_{CP} = 2.8, CH), 122.43 (dd, J_{CP} = 55.4 and 4.6, CH), 121.43 (d, J_{CP} = 21.0, C), 120.45 (d, J_{CP} = 3.3, CH), 26.82 (dd, J_{CP} = 18.2 and 4.0, CHMe₂), 18.92 (d, J_{CP} = 7.3, CHMe₂), 18.41 (d, J_{CP} = 2.3, CHMe₂). Anal. Calcd for C₃₂H₃₃NNiO₂P₂: C, 65.77; H, 5.69; N, 2.40. Found: C, 65.53; H, 5.30; N, 2.24.

Synthesis of $[\mathbf{H-1c}]Ni(CO)_2$ (2c**).** Isolated as pale yellow crystals suitable for X-ray diffraction analysis by slow evaporation of a concentrated benzene/THF solution at room temperature; yield 97%. ¹H NMR (C₆D₆, 500 MHz) δ 10.65 (t, 1, J_{HP} = 11.5, NH), 7.29 (dd, 2, Ar), 7.14 (ddd, 2, Ar), 7.10 (t, 2, Ar), 6.84 (t, 2, Ar), 2.12 (m, 4,

CHMe₂), 1.05 (dd, 12, CHMe₂), 0.93 (dd, 12, CHMe₂). ³¹P{¹H} NMR (C₆D₆, 202 MHz) δ 19.25. ¹³C{¹H} NMR (C₆D₆, 125.7 MHz) δ 201.65 (t, ²J_{CP} = 5.0, NiCO), 150.86 (t, J_{CP} = 5.0, C), 132.81 (s, CH), 130.73 (s, CH), 121.10 (t, J_{CP} = 1.4, CH), 119.54 (t, J_{CP} = 1.8, CH), 117.32 (dt, J_{CP} = 19.2, C), 26.84 (dd, CHMe₂), 18.96 (t, J_{CP} = 5.4, CHMe₂), 17.74 (s, CHMe₂). Anal. Calcd for C₂₆H₃₉NNiO₂P₂: C, 60.47; H, 7.23; N, 2.71. Found: C, 60.48; H, 6.96; N, 2.66.

Synthesis of [H·1d]Ni(CO)₂ (2d). Isolated as a pale yellow crystalline solid; yield 89%. ¹H NMR (C₆D₆, 500 MHz) δ 10.63 (t, 1, J_{HP} = 12.0, NH), 7.36 (d, 2, Ar), 7.35 (d, 2, Ar), 7.13 (t, 2, Ar), 6.89 (t, 2, Ar), 2.13 (m, 4, Cy), 1.93 (d, 4, Cy), 1.73 (d, 4, Cy), 1.63 (d, 8, Cy), 1.45 (m, 12, Cy), 1.19 (m, 8, Cy), 1.03 (m, 4, Cy). ³¹P{¹H} NMR (C₆D₆, 202 MHz) δ 9.77. ¹³C{¹H} NMR (C₆D₆, 125.7 MHz) δ 201.86 (t, ²J_{CP} = 5.5, NiCO), 151.11 (m, C), 132.64 (s, CH), 130.66 (s, CH), 121.14 (s, CH), 119.85 (s, CH), 117.81 (m, C), 36.86 (m, PCH), 29.04 (t, J_{CP} = 3.1, CH₂), 27.87 (m, CH₂), 27.65 (s, CH₂), 27.59 (m, CH₂), 26.84 (s, CH₂). Anal. Calcd for C₃₈H₅₃NNiO₂P₂: C, 67.45; H, 7.90; N, 2.07. Found: C, 67.50; H, 7.94; N, 1.86.

Synthesis of [1b]Ni(O)Me (3b). Isolated as yellow crystals suitable for X-ray diffraction analysis by layering diethyl ether on a concentrated THF solution at -35 °C; yield 92%. ¹H NMR (C₆D₆, 500 MHz) δ 7.84 (br m, 4, Ar), 7.77 (dd, 1, Ar), 7.62 (dd, 1, Ar), 7.12 (dt, 1, Ar), 7.01 (m, 7, Ar), 6.96 (dt, 1, Ar), 6.93 (dt, 1, Ar), 6.49 (tt, 1, Ar), 6.44 (tt, 1, Ar), 2.07 (m, 2, CHMe₂), 2.06 (s, 3, NiC(O)Me), 1.23 (dd, 6, CHMe₂), 1.05 (dd, 6, CHMe₂). ³¹P{¹H} NMR (C₆D₆, 202 MHz) δ 37.84 (d, ²J_{PP} = 192.4, P^{Pr}₂), 18.25 (d, ²J_{PP} = 192.4, PPh₂). ¹³C{¹H} NMR (C₆D₆, 125.7 MHz) δ 259.69 (vt, J_{CP} = 18.8, NiC(O)), 162.51 (d, J_{CP} = 4.3, C), 162.34 (vt, J_{CP} = 3.6, C), 134.89 (s, CH), 134.07 (d, J_{CP} = 11.5, CH), 132.65 (d, J_{CP} = 12.4, CH), 132.58 (s, CH), 131.95 (d, J_{CP} = 1.9, CH), 130.61 (s, CH), 129.25 (d, J_{CP} = 9.8, CH), 128.92 (s, C), 123.78 (d, J_{CP} = 48.7, C), 120.03 (d, J_{CP} = 39.7, C), 116.68 (d, J_{CP} = 7.3, CH), 116.61 (d, J_{CP} = 9.8, CH), 116.42 (d, J_{CP} = 6.1, CH), 115.67 (d, J_{CP} = 10.4, CH), 40.49 (t, J_{CP} = 6.2, NiC(O)Me), 23.60 (br d, J_{CP} = 25.0, CHMe₂), 18.88 (br s, CHMe₂), 17.40 (s, CHMe₂). Anal. Calcd for C₃₂H₃₅NNiOP₂: C, 67.38; H, 6.19; N, 2.46. Found: C, 67.08; H, 6.43; N, 2.31.

Synthesis of [1c]Ni(O)Me (3c). Isolated as yellowish green crystals suitable for X-ray diffraction analysis by slow evaporation of a concentrated benzene solution at room temperature; yield 73%. ¹H NMR (C₆D₆, 500 MHz) δ 7.69 (d, 2, Ar), 7.00 (dt, 2, Ar), 6.92 (m, 2, Ar), 6.48 (t, 2, Ar), 2.41 (s, 3, C(O)Me), 2.19 (br m, 2, PCHMe₂), 2.02 (br m, 2, PCHMe₂), 1.23 (dd, 12, PCHMe₂), 1.06 (br m, 6, PCHMe₂), 0.98 (br m, 6, PCHMe₂). ³¹P{¹H} NMR (C₆D₆, 202 MHz) δ 35.81. ¹³C{¹H} NMR (C₆D₆, 125.7 MHz) δ 259.15 (t, J_{CP} = 20.5, NiC(O)Me), 162.99 (t, J_{CP} = 11.9, C), 132.63 (s, CH), 131.93 (s, CH), 119.93 (t, J_{CP} = 19.7, C), 116.07 (t, J_{CP} = 2.8, CH), 115.86 (t, J_{CP} = 4.2, CH), 44.17 (t, J_{CP} = 5.7, NiC(O)Me), 23.36 (m, CHMe₂), 18.90 (m, CHMe₂), 17.60 (m, CHMe₂), 17.27 (m, CHMe₂). Anal. Calcd for C₂₆H₃₉NNiOP₂: C, 62.16; H, 7.83; N, 2.79. Found: C, 62.30; H, 7.60; N, 2.78.

Synthesis of [1b]Ni(O)Et (4b). Isolated as a yellow solid; yield 82%. ¹H NMR (C₆D₆, 500 MHz) δ 7.85 (br s, 4, Ar), 7.75 (dd, 1, Ar), 7.59 (dd, 1, Ar), 7.12 (t, 1, Ar), 7.01 (m, 7, Ar), 6.93 (t, 2, Ar), 6.48 (t, 1, Ar), 6.44 (t, 1, Ar), 2.52 (q, 2, NiC(O)CH₂Me), 2.07 (m, 2, CHMe₂), 1.24 (dd, 6, CHMe₂), 1.07 (dd, 6, CHMe₂), 0.68 (t, 3, NiC(O)CH₂Me). ³¹P{¹H} NMR (C₆D₆, 202 MHz) δ 36.94 (d, ²J_{PP} = 194, P^{Pr}₂), 17.57 (d, ²J_{PP} = 194, PPh₂). ¹³C{¹H} NMR (C₆D₆, 125.7 MHz) δ 261.24 (vt, ²J_{CP} = 19.2, NiC(O)), 162.49 (dd, J_{CP} = 1.6 and 3.4, C), 162.32 (dd, J_{CP} = 2.3 and 4.0, C), 134.82 (s, CH), 134.04 (d, J_{CP} = 10.2, CH), 132.64 (d, J_{CP} = 1.6, CH), 132.62 (s, CH), 131.94 (d, J_{CP} = 1.8, CH), 130.58 (s, CH), 129.24 (d, J_{CP} = 10.2, CH), 128.62 (s, C), 124.03 (d, J_{CP} = 49.1, C), 120.11 (d, J_{CP} = 39.4, C), 116.63 (d, J_{CP} = 7.3, CH), 116.46 (d, J_{CP} = 9.0, CH), 116.32 (d, J_{CP} = 5.7, CH), 115.75 (d, J_{CP} = 9.7, CH), 47.79 (vt, J_{CP} = 5.7, NiC(O)CH₂Me), 23.68 (br d, J_{CP} = 23.5, CHMe₂), 18.92 (br s, CHMe₂), 17.35 (s, CHMe₂), 8.40 (s, NiC(O)CH₂Me). Anal. Calcd for C₃₃H₃₇NNiOP₂: C, 67.82; H, 6.39; N, 2.40. Found: C, 67.60; H, 6.55; N, 2.06.

Synthesis of [1c]Ni(O)Et (4c). Isolated as a yellowish green solid; yield 54%. ¹H NMR (C₆D₆, 500 MHz) δ 7.68 (d, 2, Ar), 7.00 (dt, 2, Ar), 6.92 (m, 2, Ar), 6.48 (t, 2, Ar), 2.88 (q, 2, CH₂Me), 2.18

(br m, 2, PCHMe₂), 2.05 (br m, 2, PCHMe₂), 1.23 (dd, 12, PCHMe₂), 1.09 (m, 9, CH₂Me and PCHMe₂), 0.99 (br m, 6, PCHMe₂). ³¹P{¹H} NMR (C₆D₆, 202 MHz) δ 35.56. ¹³C{¹H} NMR (C₆D₆, 125.7 MHz) δ 259.26 (t, J_{CP} = 20.6, NiC(O)), 163.00 (t, J_{CP} = 11.7, C), 132.63 (s, CH), 131.88 (s, CH), 120.04 (t, J_{CP} = 19.9, CH), 116.04 (t, J_{CP} = 3.5, CH), 115.89 (t, J_{CP} = 4.9, C), 51.29 (t, J_{CP} = 4.8, CH₂), 23.26 (br m, PCHMe₂), 18.90 (s, Me), 18.00 (s, Me), 17.53 (s, Me), 17.28 (s, Me), 8.16 (s, Me). Anal. Calcd for C₂₇H₄₁NNiOP₂: C, 62.80; H, 8.01; N, 2.71. Found: C, 62.73; H, 7.86; N, 2.65.

Synthesis of [1b]Ni(O)hexyl (5b). Isolated as yellow crystals suitable for X-ray diffraction analysis by slow evaporation from a concentrated benzene solution at room temperature; yield 96%. ¹H NMR (C₆D₆, 500 MHz) δ 7.85 (br s, 4, Ar), 7.75 (dd, 1, Ar), 7.59 (dd, 1, Ar), 7.11 (t, 1, Ar), 7.02 (m, 7, Ar), 6.94 (t, 2, Ar), 6.48 (t, 1, Ar), 6.45 (t, 1, Ar), 2.64 (t, 2, NiC(O)CH₂(CH₂)₄Me), 2.13 (m, 2, CHMe₂), 1.28 (m, 8, CHMe₂ and NiC(O)CH₂(CH₂)₄Me), 1.16 (m, 2, NiC(O)CH₂(CH₂)₄Me), 1.10 (m, 8, CHMe₂ and NiC(O)CH₂(CH₂)₄Me), 0.96 (m, 2, NiC(O)CH₂(CH₂)₄Me), 0.83 (t, 3, NiC(O)CH₂(CH₂)₄Me). ³¹P{¹H} NMR (C₆D₆, 202 MHz) δ 36.89 (d, ²J_{PP} = 193.4, P^{Pr}₂), 17.86 (d, ²J_{PP} = 193.4, PPh₂). ¹³C{¹H} NMR (C₆D₆, 125.7 MHz) δ 260.81 (vt, ²J_{CP} = 18.8, NiC(O)), 162.48 (vt, J_{CP} = 3.9, C), 162.31 (d, J_{CP} = 3.6, C), 134.86 (s, CH), 134.08 (s, C), 134.04 (s, C), 132.65 (d, J_{CP} = 1.9, CH), 132.61 (s, CH), 131.93 (d, J_{CP} = 1.9, CH), 130.56 (s, CH), 129.24 (d, J_{CP} = 10.0, CH), 128.92 (s, CH), 124.12 (d, J_{CP} = 48.9, C), 120.08 (d, J_{CP} = 39.8, C), 116.62 (d, J_{CP} = 6.9, CH), 116.42 (d, J_{CP} = 9.1, CH), 116.29 (d, J_{CP} = 5.9, CH), 115.78 (d, J_{CP} = 10.0, CH), 55.50 (t, J_{CP} = 5.7, NiC(O)CH₂), 32.33 (s, CH₂), 29.91 (s, CH₂), 24.30 (s, CH₂), 23.76 (d, J_{CP} = 20.0, CHMe₂), 23.30 (s, CH₂), 18.92 (d, J_{CP} = 7.2, CHMe₂), 17.39 (s, CHMe₂), 14.66 (s, NiC(O)CH₂(CH₂)₄Me). Anal. Calcd for C₃₇H₄₅NNiOP₂: C, 69.38; H, 7.09; N, 2.19. Found: C, 69.37; H, 7.05; N, 1.96.

Synthesis of [1b]Ni(O)(2-norbornyl) (6b). Isolated as reddish brown crystals suitable for X-ray diffraction analysis by layering benzene on a concentrated THF solution at room temperature; yield 81%. ¹H NMR (C₆D₆, 500 MHz) δ 7.89 (br s, 2, Ar), 7.77 (br s, 2, Ar), 7.70 (dd, 1, Ar), 7.56 (dd, 1, Ar), 7.06 (m, 2, Ar), 6.99 (m, 7, Ar), 6.89 (t, 1, Ar), 6.45 (q, 2, Ar), 2.14 (m, 2, CHMe₂), 2.01 (s, 1, norbornyl), 1.71 (s, 1, norbornyl), 1.31–1.44 (m, 8, norbornyl and CHMe₂), 1.11–1.16 (m, 8, norbornyl and CHMe₂), 1.01 (m, 2, norbornyl), 0.87 (m, 2, norbornyl), 0.80 (d, 1, norbornyl). ³¹P{¹H} NMR (C₆D₆, 202 MHz) δ 34.79 (d, ²J_{PP} = 194.2, P^{Pr}₂), 18.21 (d, ²J_{PP} = 194.2, PPh₂). ¹³C{¹H} NMR (C₆D₆, 125.7 MHz) δ 264.11 (t, J_{CP} = 18.3, NiC(O)), 162.42 (dd, J_{CP} = 3.6 and 14.0, C), 162.25 (dd, J_{CP} = 3.0 and 9.7, C), 134.52 (s, CH), 134.21 (dd, J_{CP} = 10.9 and 26.2, C), 132.80 (s, CH), 132.45 (s, CH), 131.93 (s, CH), 130.45 (d, J_{CP} = 22.5, CH), 129.20 (d, J_{CP} = 7.4, CH), 129.12 (d, J_{CP} = 7.4, CH), 125.05 (d, J_{CP} = 49.5, C), 120.24 (d, J_{CP} = 40.1, C), 116.90 (d, J_{CP} = 9.7, CH), 116.84 (d, J_{CP} = 7.2, CH), 115.79 (d, J_{CP} = 6.1, CH), 115.36 (d, J_{CP} = 9.1, CH), 65.17 (dd, J_{CP} = 3.6 and 7.2, CH), 40.06 (s, CH), 36.83 (s, CH₂), 36.73 (s, CH), 34.89 (s, CH₂), 30.65 (s, CH₂), 29.76 (s, CH₂), 24.44 (br m, CHMe₂), 19.15 (br m, CHMe₂), 17.44 (d, J_{CP} = 18.3, CHMe₂). Anal. Calcd for C₃₈H₄₃NNiOP₂: C, 70.16; H, 6.67; N, 2.15. Found: C, 69.82; H, 6.78; N, 1.78.

Synthesis of [MeC(O)N(o-C₆H₄PPh₂)₂]Ni(CO)₂ (7a). Isolated as a pale yellow solid; yield 75%. ¹H NMR (C₆D₆, 300 MHz) δ 8.08 (dd, 2, Ar), 7.93 (dd, 2, Ar), 7.42 (br s, 2, Ar), 7.10 (m, 4, Ar), 6.79–6.93 (m, 12, Ar), 6.68 (m, 4, Ar), 6.55 (t, 2, Ar), 2.22 (s, 3, C(O)Me). ³¹P{¹H} NMR (C₆D₆, 121.5 MHz) δ 23.37 (d, ²J_{PP} = 5.6), 22.16 (d, ²J_{PP} = 5.6). ¹³C{¹H} NMR (C₆D₆, 75.5 MHz) δ 202.11 (s, NiC(O)Me), 197.24 (vt, J_{CP} = 4.45, NiC(O)), 180.81 (s, C), 147.43 (d, J_{CP} = 16, C), 140.33 (d, J_{CP} = 34.43, C), 137.05 (s, C), 136.89 (d, J_{CP} = 23.25, CH), 135.43 (d, J_{CP} = 15.18, CH), 134.90 (d, J_{CP} = 16.38, CH), 134.66 (s, CH), 133.13 (d, J_{CP} = 4.83, CH), 132.33 (m, CH), 130.68 (s, CH), 130.22 (s, CH), 129.21 (m, CH), 26.72 (s, CH₃). Anal. Calcd for C₄₀H₃₁NNiO₃P₂: C, 69.18; H, 4.50; N, 2.02. Found: C, 69.01; H, 4.24; N, 2.21.

Synthesis of [EtC(O)N(o-C₆H₄PPh₂)₂]Ni(CO)₂ (8a). Isolated as pale yellow crystals suitable for X-ray diffraction analysis by slow evaporation of a concentrated benzene solution at room temperature; yield 69%. ¹H NMR (C₆D₆, 500 MHz) δ 8.05 (dd, 2, Ar), 7.93 (t, 2,

Ar), 7.25 (t, 2, Ar), 7.18 (t, 2, Ar), 7.09 (t, 2, Ar), 7.03 (t, 2, Ar), 6.92–6.98 (m, 6, Ar), 6.81–6.88 (m, 6, Ar), 6.71 (m, 4, Ar), 2.29 (qd, 1, $^2J_{\text{HAHB}} = 17$, $^3J_{\text{HAMe}} = 7$, C(O)CH₂H_BMe), 2.16 (qd, 1, $^2J_{\text{HAHB}} = 17$, $^3J_{\text{HBMe}} = 7$, C(O)CH₂H_BMe), 0.93 (t, 3, CH₂Me). $^{31}\text{P}\{^1\text{H}\}$ NMR (C₆D₆, 202 MHz) δ 24.72 (d, $^2J_{\text{PP}} = 5.5$), 23.54 (d, $^2J_{\text{PP}} = 5.5$). $^{13}\text{C}\{^1\text{H}\}$ NMR (C₆D₆, 125.7 MHz) 202.50 (s, NC(O)Et), 197.93 (vt, $J_{\text{CP}} = 6.0$, NiCO), 175.32 (s, C), 148.43 (dd, $J_{\text{CP}} = 90.6$ and 16.4, C), 141.65 (d, $J_{\text{CP}} = 16.5$, C), 139.73 (dd, $J_{\text{CP}} = 30.8$ and 12.9, C), 137.57 (d, $J_{\text{CP}} = 31.6$, C), 137.22 (s, CH), 136.25 (dd, $J_{\text{CP}} = 27.1$ and 2.7, C), 135.97 (s, CH), 135.47 (d, $J_{\text{CP}} = 15.0$, CH), 134.68 (d, $J_{\text{CP}} = 16.0$, CH), 134.58 (d, $J_{\text{CP}} = 25.2$, C), 134.38 (t, $J_{\text{CP}} = 5.9$, CH), 133.79 (d, $J_{\text{CP}} = 22.5$, C), 133.10 (d, $J_{\text{CP}} = 12.8$, CH), 132.50 (d, $J_{\text{CP}} = 12.3$, CH), 132.13 (d, $J_{\text{CP}} = 5.0$, CH), 130.99 (s, CH), 130.33 (s, CH), 130.16 (s, CH), 129.98 (d, $J_{\text{CP}} = 5.5$, CH), 129.29 (vt, $J_{\text{CP}} = 5.0$, CH), 129.05 (d, $J_{\text{CP}} = 9.1$, CH), 128.92 (s, CH), 128.69 (s, CH), 128.53 (m, CH), 128.33 (d, $J_{\text{CP}} = 8.3$, CH), 128.18 (m, CH), 126.14 (d, $J_{\text{CP}} = 3.6$, CH), 31.09 (s, CH₂), 10.04 (s, CH₃). Anal. Calcd for C₄₁H₃₃NNiO₃P₂: C, 69.50; H, 4.70; N, 1.98. Found: C, 69.76; H, 4.40; N, 2.16.

Synthesis of [1a]Ni[C(O)NHPH] (9a). Isolated as red crystals suitable for X-ray diffraction analysis by cooling a concentrated THF solution to -35 °C; yield 92%. ^1H NMR (C₆D₆, 500 MHz) δ 7.79 (d, 8, Ar), 7.10 (m, 1, Ar), 6.96 (m, 20, Ar), 6.77 (s, 1, NH), 6.71 (t, 2, Ar), 6.44 (t, 2, Ar). $^{31}\text{P}\{^1\text{H}\}$ NMR (C₆D₆, 202 MHz) δ 22.25. $^{13}\text{C}\{^1\text{H}\}$ NMR (C₆D₆, 125.7 MHz) δ 194.48 (t, $^2J_{\text{CP}} = 31.0$, NiC(O)NHPH), 162.30 (t, $J_{\text{CP}} = 13.8$, C), 139.92 (s, C), 135.05 (s, CH), 134.28 (t, $J_{\text{CP}} = 6.5$, CH), 132.64 (s, CH), 131.71 (t, $J_{\text{CP}} = 23.8$, C), 130.72 (s, CH), 129.30 (t, $J_{\text{CP}} = 4.6$, CH), 128.99 (s, CH), 123.78 (t, $J_{\text{CP}} = 23.7$, C), 122.43 (s, CH), 118.43 (s, CH), 117.57 (t, $J_{\text{CP}} = 3.6$, CH), 116.49 (t, $J_{\text{CP}} = 4.5$, CH). Anal. Calcd for C₄₃H₃₄N₂NiOP₂: C, 72.18; H, 4.79; N, 3.92. Found: C, 71.98; H, 4.68; N, 3.95.

Synthesis of [1c]Ni[C(O)NHPH] (9c). Isolated as yellow crystals suitable for X-ray diffraction analysis by slow evaporation of a concentrated benzene solution at room temperature; yield 78%. ^1H NMR (C₆D₆, 500 MHz) δ 7.73 (d, 2, Ar), 7.59 (d, 2, Ar), 7.19 (s, 1, NH), 7.15 (m, 2, Ar), 7.01 (t, 2, Ar), 6.97 (m, 2, Ar), 6.85 (t, 1, Ar), 6.50 (t, 2, Ar), 2.29 (m, 2, PCHMe₂), 2.13 (m, 2, PCHMe₂), 1.31 (m, 6, PCHMe₂), 1.21 (m, 6, PCHMe₂), 1.09 (m, 6, PCHMe₂), 1.02 (m, 6, PCHMe₂). $^{31}\text{P}\{^1\text{H}\}$ NMR (C₆D₆, 202 MHz) δ 40.87. $^{13}\text{C}\{^1\text{H}\}$ NMR (C₆D₆, 125.7 MHz) δ 196.13 (t, $J_{\text{CP}} = 27.4$, NiC(O)NHPH), 163.46 (t, $J_{\text{CP}} = 11.9$, C), 139.49 (s, ipso-NHPH), 132.83 (s, CH), 132.01 (s, CH), 129.76 (s, CH), 122.70 (s, CH), 120.58 (t, $J_{\text{CP}} = 18.7$, C), 118.37 (s, CH), 116.45 (t, $J_{\text{CP}} = 3.2$, CH), 115.96 (t, $J_{\text{CP}} = 4.6$, CH), 23.70 (m, CHMe₂), 18.74 (s, CHMe₂), 18.00 (br s, CHMe₂), 17.26 (br s, CHMe₂). Anal. Calcd for C₃₁H₄₂N₂NiOP₂: C, 64.25; H, 7.31; N, 4.84. Found: C, 63.96; H, 7.44; N, 4.46.

■ ASSOCIATED CONTENT

Supporting Information

X-ray crystallographic data for **2b**, **2c**, **3b**, **3c**, **5b**, **6b**, **8a**, **9a**, **9c**, and **[1b]NiMe**; molecular structures of **2c**, **9c**, and **[1b]NiMe**. This material is available free of charge via the Internet at <http://pubs.acs.org>.

■ AUTHOR INFORMATION

Corresponding Author

*E-mail: lcliang@mail.nsysu.edu.tw.

■ ACKNOWLEDGMENTS

We thank the National Science Council of Taiwan for financial support (NSC 99-2113-M-110-003-MY3 and 99-2119-M-110-002), Mr. Ting-Shen Kuo (NTNU) for assistance with X-ray crystallography, and the National Center for High-performance Computing (NCHC) for the access to chemical databases.

■ REFERENCES

- Hebrard, F.; Kalck, P. *Chem. Rev.* **2009**, *109*, 4272–4282.
- Drent, E.; Budzelaar, P. H. M. *Chem. Rev.* **1996**, *96*, 663–681.
- Sen, A. *Acc. Chem. Res.* **1993**, *26*, 303–310.
- Rix, F. C.; Brookhart, M.; White, P. S. *J. Am. Chem. Soc.* **1996**, *118*, 4746–4764.
- Nakamura, A.; Munakata, K.; Ito, S.; Kochi, T.; Chung, L. W.; Morokuma, K.; Nozaki, K. *J. Am. Chem. Soc.* **2011**, *133*, 6761–6779.
- Christophe, M.; Thomas, C. M.; Süß-Fink, G. *Coord. Chem. Rev.* **2003**, *243*, 125–142.
- Ford, P. C. *Acc. Chem. Res.* **1981**, *14*, 31–37.
- Hegg, E. L. *Acc. Chem. Res.* **2004**, *37*, 775–783.
- Stavropoulos, P.; Carrie, M.; Muetterties, M. C.; Holm, R. H. *J. Am. Chem. Soc.* **1990**, *112*, 5385–5387.
- Ariyananda, P. W. G.; Kieber-Emmons, M. T.; Yap, G. P. A.; Riordan, C. G. *Dalton Trans.* **2009**, 4359–4369.
- Martinelli, J. R.; Freckmann, D. M. M.; Buchwald, S. L. *Org. Lett.* **2006**, *8*, 4843–4846.
- Kramer, J. W.; Lobkovsky, E. B.; Coates, G. W. *Org. Lett.* **2006**, *8*, 3709–3712.
- Rayabarapu, D. K.; Cheng, C.-H. *J. Am. Chem. Soc.* **2002**, *124*, 5630–5631.
- Rowley, J. M.; Lobkovsky, E. B.; Coates, G. W. *J. Am. Chem. Soc.* **2007**, *129*, 4948–4960.
- Brummond, K. M.; Gao, D. *Org. Lett.* **2003**, *5*, 3491–3494.
- García-Gómez, G.; Moretó, J. M. *J. Am. Chem. Soc.* **1999**, *121*, 878–879.
- Jacob, J.; Reynolds, K. A.; Jones, W. D.; Godleski, S. A.; Valente, R. R. *Organometallics* **2001**, *20*, 1028–1031.
- Liang, L.-C. *Coord. Chem. Rev.* **2006**, *250*, 1152–1177.
- Liang, L.-C.; Lin, J.-M.; Lee, W.-Y. *Chem. Commun.* **2005**, 2462–2464.
- Liang, L.-C.; Chien, P.-S.; Huang, M.-H. *Organometallics* **2005**, *24*, 353–357.
- Liang, L.-C.; Lee, W.-Y.; Tsai, T.-L.; Hsu, Y.-L.; Lee, T.-Y. *Dalton Trans.* **2010**, 39, 8748–8758.
- Liang, L.-C.; Lee, W.-Y.; Yin, C.-C. *Organometallics* **2004**, *23*, 3538–3547.
- Liang, L.-C.; Chien, P.-S.; Hsiao, Y.-C.; Li, C.-W.; Chang, C.-H. *J. Organomet. Chem.* **2011**, *696*, 3961–3965.
- Lee, P.-Y.; Liang, L.-C. *Inorg. Chem.* **2009**, *48*, 5480–5487.
- Chien, P.-S.; Liang, L.-C. *Inorg. Chem.* **2005**, *44*, 5147–5151.
- Liang, L.-C.; Huang, M.-H.; Hung, C.-H. *Inorg. Chem.* **2004**, *43*, 2166–2174.
- Huang, M.-H.; Liang, L.-C. *Organometallics* **2004**, *23*, 2813–2816.
- Liang, L.-C.; Lee, W.-Y.; Hung, C.-H. *Inorg. Chem.* **2003**, *42*, 5471–5473.
- Winter, A. M.; Eichele, K.; Mack, H. G.; Potuznik, S.; Mayer, H. A.; Kaska, W. C. *J. Organomet. Chem.* **2003**, *682*, 149–154.
- Menard, G.; Jong, H.; Fryzuk, M. D. *Organometallics* **2009**, *28*, 5253–5260.
- MacLachlan, E. A.; Hess, F. M.; Patrick, B. O.; Fryzuk, M. D. *J. Am. Chem. Soc.* **2007**, *129*, 10895–10905.
- MacLachlan, E. A.; Fryzuk, M. D. *Organometallics* **2005**, *24*, 1112–1118.
- Yurkerwich, K.; Parkin, G. *Inorg. Chim. Acta* **2010**, *364*, 157–161.
- Ozerov, O. V. In *The Chemistry of Pincer Compounds*; Morales-Morales, D., Jensen, C. M., Eds.; Elsevier: Amsterdam, 2007, p 287–309.
- Fafard, C. M.; Adhikari, D.; Foxman, B. M.; Mindiola, D. J.; Ozerov, O. V. *J. Am. Chem. Soc.* **2007**, *129*, 10318–10319.
- Cavaliere, V. N.; Crestani, M. G.; Pinter, B.; Pink, M.; Chen, C. H.; Baik, M. H.; Mindiola, D. J. *J. Am. Chem. Soc.* **2011**, *133*, 10700–10703.
- Andino, J. G.; Kilgore, U. J.; Pink, M.; Ozarowski, A.; Krzystek, J.; Telsler, J.; Baik, M. H.; Mindiola, D. J. *Chem. Sci.* **2010**, *1*, 351–356.
- Adhikari, D.; Pink, M.; Mindiola, D. J. *Organometallics* **2009**, *28*, 2072–2077.

- (39) Adhikari, D.; Mossin, S.; Basuli, F.; Dible, B. R.; Chipara, M.; Fan, H.; Huffman, J. C.; Meyer, K.; Mendiola, D. J. *Inorg. Chem.* **2008**, *47*, 10479–10490.
- (40) Harkins, S. B.; Peters, J. C. *J. Am. Chem. Soc.* **2005**, *127*, 2030–2031.
- (41) Mankad, N. P.; Harkins, S. B.; Antholine, W. E.; Peters, J. C. *Inorg. Chem.* **2009**, *48*, 7026–7032.
- (42) Whited, M. T.; Grubbs, R. H. *Acc. Chem. Res.* **2009**, *42*, 1607–1616.
- (43) Whited, M. T.; Grubbs, R. H. *J. Am. Chem. Soc.* **2008**, *130*, 5874–5875.
- (44) Whited, M. T.; Grubbs, R. H. *J. Am. Chem. Soc.* **2008**, *130*, 16476–16477.
- (45) Calimano, E.; Tilley, T. D. *J. Am. Chem. Soc.* **2009**, *131*, 11161–11173.
- (46) Cantat, T.; Scott, B. L.; Morris, D. E.; Kiplinger, J. L. *Inorg. Chem.* **2009**, *48*, 2114–2127.
- (47) Liang, L.-C.; Chien, P.-S.; Lee, P.-Y. *Organometallics* **2008**, *27*, 3082–3093.
- (48) Liang, L.-C.; Lin, J.-M.; Hung, C.-H. *Organometallics* **2003**, *22*, 3007–3009.
- (49) Liang, L.-C.; Chien, P.-S.; Lin, J.-M.; Huang, M.-H.; Huang, Y.-L.; Liao, J.-H. *Organometallics* **2006**, *25*, 1399–1411.
- (50) Fryzuk, M. D.; Macneil, P. A.; Rettig, S. J. *J. Organomet. Chem.* **1987**, *332*, 345–360.
- (51) Fryzuk, M. D.; Macneil, P. A. *Organometallics* **1982**, *1*, 1540–1541.
- (52) Fryzuk, M. D.; Macneil, P. A. *J. Am. Chem. Soc.* **1984**, *106*, 6993–6999.
- (53) Liang, L.-C.; Chien, P.-S.; Huang, Y.-L. *J. Am. Chem. Soc.* **2006**, *128*, 15562–15563.
- (54) Casey, C. P.; Neumann, S. M. *J. Am. Chem. Soc.* **1976**, *98*, 5395–5396.
- (55) Tam, W.; Wong, W.-K.; Gladysz, J. A. *J. Am. Chem. Soc.* **1979**, *101*, 1589–1591.
- (56) Bianchini, C.; Meli, A. *Organometallics* **1985**, *4*, 1537–1542.
- (57) Fryzuk, M. D.; Mylvaganam, M.; Zaworotko, M. J.; MacGillivray, L. R. *Organometallics* **1996**, *15*, 1134–1138.
- (58) Liang, L.-C.; Li, C.-W.; Lee, P.-Y.; Chang, C.-H.; Lee, H. M. *Dalton Trans.* **2011**, *40*, 9004–9011.
- (59) Darensbourg, D. J.; Robertson, J. B.; Larkins, D. L.; Reibenspies, J. H. *Inorg. Chem.* **1999**, *38*, 2473–2481.
- (60) Lesueur, W.; Solari, E.; Floriani, C.; ChiesiVilla, A.; Rizzoli, C. *Inorg. Chem.* **1997**, *36*, 3354–3362.
- (61) Oxidative addition of N-C_{sp}³ to low valent groups 9 and 10 metals is known; for instance, see: (a) Ozerov, O. V.; Guo, C. Y.; Fan, L.; Foxman, B. M. *Organometallics* **2004**, *23*, 5573–5580. (b) Fan, L.; Yang, L.; Guo, C. Y.; Foxman, B. M.; Ozerov, O. V. *Organometallics* **2004**, *23*, 4778–4787. (c) Weng, W.; Guo, C. Y.; Moura, C.; Yang, L.; Foxman, B. M.; Ozerov, O. V. *Organometallics* **2005**, *24*, 3487–3499. (d) Ozerov, O. V.; Guo, C. Y.; Papkov, V. A.; Foxman, B. M. *J. Am. Chem. Soc.* **2004**, *126*, 4792–4793.
- (62) For instance, upon carbonylation of [1c]NiPh in benzene at ambient conditions, a new singlet resonance at 34.7 ppm, ascribed tentatively to [1c]NiC(O)Ph, begins to appear cleanly after 3 days (10% conversion) in the ³¹P{¹H} NMR spectrum.
- (63) For representative precedents of kinetic and thermodynamic studies of carbonylation or decarbonylation involving metal–alkyl versus metal–aryl bonds, see: (a) ref 50. (b) Otsuka, S.; Nakamura, A.; Yoshida, T.; Naruto, M.; Ataka, K. *J. Am. Chem. Soc.* **1973**, *95*, 3180–3188. (c) Whited, M. T.; Zhu, Y. J.; Timpa, S. D.; Chen, C. H.; Foxman, B. M.; Ozerov, O. V.; Grubbs, R. H. *Organometallics* **2009**, *28*, 4560–4570. (d) Keim, W.; Behr, A.; Gruber, B.; Hoffmann, B.; Kowaldt, F. H.; Kurschner, U.; Limbacher, B.; Sistig, F. P. *Organometallics* **1986**, *5*, 2356–2359.
- (64) Shultz, C. S.; DeSimone, J. M.; Brookhart, M. *J. Am. Chem. Soc.* **2001**, *123*, 9172–9173.
- (65) To compare with **3b**, the X-ray structure of [1b]NiMe was characterized; see Supporting Information.
- (66) Liang, L.-C.; Chien, P.-S.; Lee, P.-Y.; Lin, J.-M.; Huang, Y.-L. *Dalton Trans.* **2008**, 3320–3327.
- (67) Holland, P. L.; Andersen, R. A.; Bergman, R. G. *J. Am. Chem. Soc.* **1996**, *118*, 1092–1104.
- (68) Mendiola, D. J.; Hillhouse, G. L. *Chem. Commun.* **2002**, 1840–1841.
- (69) Sheldrick, G. M. *SHELXTL*, version 5.1; Bruker AXA Inc.: Madison, WI, 1998.